A statistically accurate modified quasilinear Gaussian closure for uncertainty quantification in turbulent dynamical systems

Themistoklis P. Sapsis and Andrew J. Majda
Courant Institute of Mathematical Sciences, New York University
251 Mercer str., New York, 10012 NY

July 23, 2012

Abstract

We develop a novel second-order closure methodology for uncertainty quantification in damped forced nonlinear systems with high dimensional phase-space that possess a high-dimensional chaotic attractor. We focus on turbulent systems with quadratic nonlinearities where the finite size of the attractor is caused exclusively by the synergistic activity of persistent, linearly unstable directions and a nonlinear energy transfer mechanism. We first illustrate how existing UQ schemes that rely on the Gaussian assumption will fail to perform reliable UQ in the presence of unstable dynamics. To overcome these difficulties, a modified quasilinear Gaussian (MQG) closure is developed in two stages. First we exploit exact statistical relations between second order correlations and third order moments in statistical equilibrium in order to decompose the energy flux at equilibrium into precise additional damping and enhanced noise on suitable modes, while preserving statistical symmetries; in the second stage, we develop a nonlinear MQG dynamical closure which has this statistical equilibrium behavior as a stable fixed point of the dynamics. Our analysis, UQ schemes, and conclusions are illustrated through a specific toy-model, the forty-modes Lorenz 96 system, which despite its simple formulation, presents strongly turbulent behavior with a large number of unstable dynamical components in a variety of chaotic regimes. A suitable version of MQG successfully captures the mean and variance, in transient dynamics with initial data far from equilibrium and with large random fluctuations in forcing, very cheaply at the cost of roughly two ensemble members in a Monte-Carlo simulation.

1 Introduction

Turbulent dynamical systems have been a center of research activity for many decades and this is both due to the mathematical challenges associated with them but also due to their importance on many fields of nature and technology such as prediction in geosciences, flow optimization and design in engineering, and electrical flow prediction in neural science, just to mention a few. By using the term 'Turbulent Dynamical Systems' we refer to complex systems that evolve in time and 'live' in high dimensional phase spaces, having a large number of internal instabilities acting, in general, over different temporal and spatial scales and ultimately lead to strong nonlinear energy

transfers between modes. These internal instabilities cause rapid growth of small uncertainties which inevitably exist in the initial conditions, the system parameters, and the modeling equations such as uncertainty in the forcing.

The above challenges lead naturally to the adoption of a statistical framework where the goal now is to model and quantify uncertainty rather than trying to 'avoid' it. Here we will mainly focus on uncertainty quantification schemes for turbulent systems with quadratic nonlinearities and spatially homogeneous statistics motivated by the corresponding problems in fluid flows. In this case a turbulent regime is characterized by distribution of non-negligible amounts of energy over a large (if not infinite) number of modes including the stable ones. This wide distribution of energy over phase space is due to the large number of linearly unstable modes that continuously amplify volumes in phase space. Obviously for a linear system, the presence of persistent instabilities would ultimately lead to energy blow-ups. However, for a nonlinear turbulent system this is not the case since the synergistic activity of nonlinear dynamical effects and persistent linear instabilities creates a continuous transfer of energy from the unstable to the stable modes - a mechanism that has as a result the wide distribution of energy over stable and unstable modes.

The goal of this work is first to emphasize some important features of turbulent systems (with quadratic nonlinearities) associated with their dynamical and energy-transfer mechanisms. Based on these properties we will then demonstrate some fundamental limitations that widely-used UQ schemes posses in turbulent regimes. Particular emphasis will be given on UQ closure schemes based on partial linearization of the dynamics or Gaussian closure of the infinite system of moment equations.

Motivated by this discussion we will then develop a novel, second-order, closure scheme based on the direct modeling of the nonlinear energy fluxes which are connected with higher-order statistics. More specifically by using just second-order information for the statistical steady state we will give explicit expressions for the nonlinear fluxes which i) are consistent with the dynamical properties of the exact nonlinear fluxes, ii) reproduce the correct steady state information (both in terms of energy and stability), iii) are parametrized with respect to instantaneous spatial system properties (such as total energy) in order to achieve correct temporal scales in the response.

Essentially, we will model the effect of the nonlinear energy transfers on each mode by i) adding to the linearly unstable modes systematically additional damping which will account for the departure of energy due to nonlinear terms (balancing the linearly unstable character of these modes), and ii) adding to the linearly stable modes additional stochastic excitation which will model the energy received by the unstable modes. The additional damping and stochastic excitation will be added in a dynamically consistent way in order to satisfy the properties and symmetries of the nonlinear fluxes produced by the third-order statistics (even though we will not use statistics beyond second order in our analysis). The relative magnitude of the additional damping and noise for each mode will be dictated by the second-order, steady state, statistical information and will be parametrized by a suitable spatial functional of the statistics that follows from scaling arguments.

Through this approach we will create a nonlinear model with the minimal additional damping and additional stochastic forcing required to reproduce as stable solution the correct energy distribution of the system in steady state. Moreover, because of the parametrization employed in the nonlinear fluxes, their dynamically consistent form, and the fact that the linear part in the approximation scheme is exact, we will see that the developed UQ scheme performs impressively even in energetic regimes which are completely different from the steady-state. This is also the case when the forcing parameters are different from those used to compute the steady state statistics, time-dependent, and do not allow the system to reach a statistichal equilibrium.

For illustration, validation, and comparison purposes we will use the Lorenz 96 system (L-96) which is the simplest paradigm of a complex turbulent dynamical systems possessing properties found in realistic turbulent systems such as, energy-preserving advection, damping and forcing. From the point of view of statistical properties the turbulent responses of L-96 are characterized by important energy spanning the whole spectrum, a large number of persistent instabilities, and strong nonlinear energy transfers between modes. Therefore, L-96 is a perfect candidate both to illustrate the limitations of existing UQ schemes which are based on Gaussian closure but also to validate the derived UQ model.

2 Turbulent systems with quadratic nonlinearities

We start by providing the general setup which will be a high dimensional system with linear dynamics and an energy preserving quadratic part. More specifically, the general system that we will consider for our analysis is given by

$$\frac{d\mathbf{u}}{dt} = \mathcal{L}\left[\mathbf{u}\right] \equiv \left[L + D\right]\mathbf{u} + B\left(\mathbf{u},\mathbf{u}\right) + \mathbf{F}\left(t\right) + \dot{W}_k\left(t;\omega\right)\sigma_k\left(t\right) \tag{1}$$

acting on $\mathbf{u} \in \mathbb{R}^N$. In the above equation we have:

- L being a skew-symmetric linear operator representing the $\beta-$effect of Earth's curvature, topology etc. and satisfying,
$$L^* = -L.$$
- D being a negative definite symmetric operator,
$$D^* = D,$$
representing dissipative processes such as surface drag, radiative damping, viscosity, etc.

The quadratic operator $B\left(\mathbf{u},\mathbf{u}\right)$ conserves the energy by itself so that it satisfies

$$B\left(\mathbf{u},\mathbf{u}\right).\mathbf{u} = 0.$$

Finally, $\mathbf{F}\left(\mathbf{x},t\right) + \dot{W}_k\left(t;\omega\right)\sigma_k\left(\mathbf{x},t\right)$ represents the effect of external forcing i.e. solar forcing, which we will assume that it can be split into a mean component $\mathbf{F}\left(\mathbf{x},t\right)$ and a stochastic component with white noise characteristics.

We use a finite-dimensional representation of the stochastic field consisting of fixed-in-time, $M-$dimensional, orthonormal basis (where M can be relatively large)

$$\mathbf{u}\left(t\right) = \bar{\mathbf{u}}\left(t\right) + Z_i\left(t;\omega\right)\mathbf{v}_i.$$

where $\bar{\mathbf{u}}\left(t\right)$ represent the ensemble average of the response, i.e. the mean field, and $Z_i\left(t;\omega\right)$ are stochastic processes.

The mean field equation is given by

$$\frac{d\bar{\mathbf{u}}}{dt} = \left[L + D\right]\bar{\mathbf{u}} + B(\bar{\mathbf{u}},\bar{\mathbf{u}}) + R_{ij}B\left(\mathbf{v}_i,\mathbf{v}_j\right) + \mathbf{F}. \tag{2}$$

Moreover the random component of the solution, $\mathbf{u}' = Z_i(t;\omega)\,\mathbf{v}_i$ satisfies

$$\frac{d\mathbf{u}'}{dt} = [L+D]\,\mathbf{u}' + B(\bar{\mathbf{u}},\mathbf{u}') + B(\mathbf{u}',\bar{\mathbf{u}}) + B(\mathbf{u}',\mathbf{u}') + \dot{W}_k(t;\omega)\,\sigma_k(t) \tag{3}$$

By projecting the above equation to each basis element $\mathbf{v}_i$ we obtain

$$\frac{dZ_i}{dt} = Z_j\left([L+D]\,\mathbf{v}_j + B(\bar{\mathbf{u}},\mathbf{v}_j) + B(\mathbf{v}_j,\bar{\mathbf{u}})\right).\mathbf{v}_i + B(\mathbf{u}',\mathbf{u}').\mathbf{v}_i + \dot{W}_k\sigma_k.\mathbf{v}_i$$

From the last equation we directly obtain the evolution of the covariance matrix $R = \langle \mathbf{Z}\mathbf{Z}^* \rangle$

$$\frac{dR}{dt} = L_v R + R L_v^* + Q_F + Q_\sigma, \tag{4}$$

where we have:

i) the linear dynamics operator expressing energy transfers between the mean field and the stochastic modes (effect due to B), as well as energy dissipation (effect due to D) and non-normal dynamics (effect due to L)

$$\{L_v\}_{ij} = \left([L+D]\,\mathbf{v}_j + B(\bar{\mathbf{u}},\mathbf{v}_j) + B(\mathbf{v}_j,\bar{\mathbf{u}})\right).\mathbf{v}_i \tag{5}$$

ii) the positive definite operator expressing energy transfer due to external stochastic forcing

$$\{Q_\sigma\}_{ij} = (\mathbf{v}_i.\sigma_k)\,(\sigma_k.\mathbf{v}_j). \tag{6}$$

iii) as well as the energy flux between different modes due to non-Gaussian statistics (or nonlinear terms) modeled through third-order moments

$$Q_F = \overline{Z_m Z_n Z_j} B(\mathbf{v}_m,\mathbf{v}_n).\mathbf{v}_i + \overline{Z_m Z_n Z_i} B(\mathbf{v}_m,\mathbf{v}_n).\mathbf{v}_j \tag{7}$$

The last term involves higher-order statistics and therefore suitable closure assumtpions need to be made in order to setup a UQ scheme. Moreover, the energy conservation property of the quadratic operator B is inhereted by the matrix Q_F since

$$Tr[Q_F] = 2\overline{Z_m Z_n Z_i} B(\mathbf{v}_m,\mathbf{v}_n).\mathbf{v}_i \tag{8}$$

$$= 2B(Z_m\mathbf{v}_m, Z_n\mathbf{v}_n).Z_i\mathbf{v}_i = 2B(\mathbf{u}',\mathbf{u}').\mathbf{u}' = 0 \tag{9}$$

The above exact statistical equations will be the starting point for the approximation schemes that we will present and develop below.

2.1 The Lorenz 96 system

The simplest prototype example of a turbulent dynamical system is due to Lorenz and is called the Lorenz 96 (L-96) model. It is widely used as a test model for algorithms for prediction, filtering, and low frequency climate response [7, 8, 9, 12, 11]. The L-96 model is a discrete periodic model given by the following system

$$\frac{du_i}{dt} = u_{i-1}(u_{i+1} - u_{i-2}) - u_i + F, \qquad i = 0, ..., J-1 \tag{10}$$

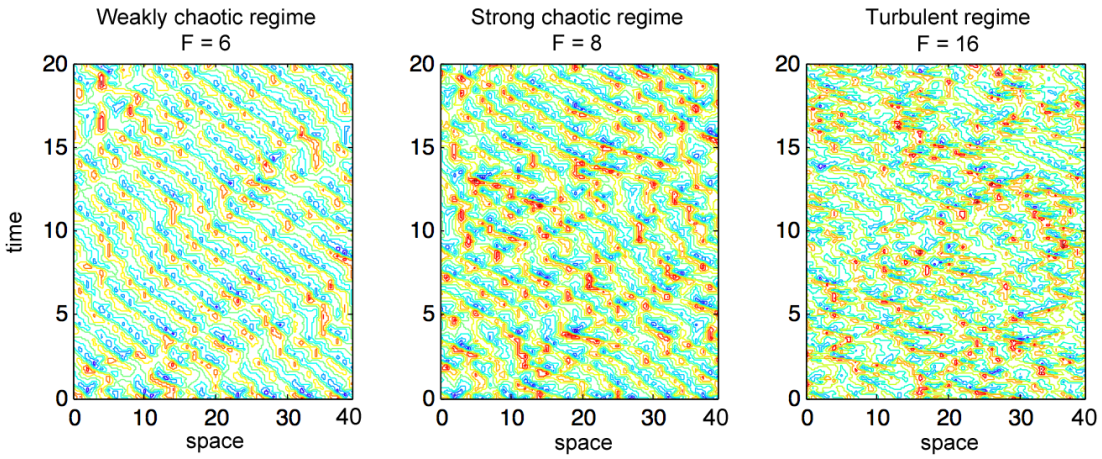

Figure 1: Space-time of numerical solutions of L-96 model for weakly chaotic ($F = 6$), strongly chaotic ($F = 8$), and fully turbulent ($F = 16$) regime.

with $J = 40$ and with F the deterministic forcing parameter. We can easily observe that the energy conservation property for the quadratic part is satisfied (i.e. $B(\mathbf{u}, \mathbf{u}) .\mathbf{u} = \mathbf{0}$) and the negative definite part has the diagonal form $\mathbf{D} = -\mathbf{I}$.

The model is designed to mimic baroclinic turbulence in the midlatitude atmosphere with the effects of energy conserving nonlinear advection and dissipation represented by the first two terms in (10). For sufficiently strong forcing values such as $F = 6, 8$ or 16 the L-96 is a prototype turbulent dynamical system which exhibits features of weakly chaotic turbulence ($F = 6$), strong chaotic turbulence ($F = 8$), and strong turbulence ($F = 16$) (cf. Figure 1).

Since the L-96 system is invariant under translations we will use the Fourier modes as a fixed basis to describe its dynamics. Because of the translation invariance property the statistics in the steady state will be spatially homogeneous, i.e. the mean field will be spatially constant and the covariance operator will have a diagonal form. In addition if the initial conditions are spatially homogeneous the above properties will hold over the whole duration of the responce. Although spatial homogeneity simplifies the technicalities of our analysis, the majority of our conclusions extend to the non-homogeneous case as shown in Figure 10 below.

In the L-96 system the external noise is zero, and therefore we have no contribution from external noise in eq. (4), i.e. $Q_\sigma = 0$. Thus uncertainty can only build-up from the unstable modes of the linearized dynamics - described by $L_v(\bar{\mathbf{u}})$ - which will magnify the initial uncertainty. In Figure 2 we present the number of unstable wavenumbers, i.e. the number of eigenvalue pairs with positive real part for the linearized matrix $L_v(\bar{\mathbf{u}})$, with respect to the value of the steady state mean field (note that spatial homogeneity implies spatially constant mean field). In the same plot we show the with dashed lines the steady state value of the mean field for specific values of the forcing parameter F. Based on the presence of persistent positive eigenvalues in the steady-state we have (for sufficiently large F) the following energy cycle (Figure 3):

1. Energy from the external excitation F leads to the growth of the mean field energy $\frac{1}{2}\bar{\mathbf{u}}.\bar{\mathbf{u}}$ (equation (2)).

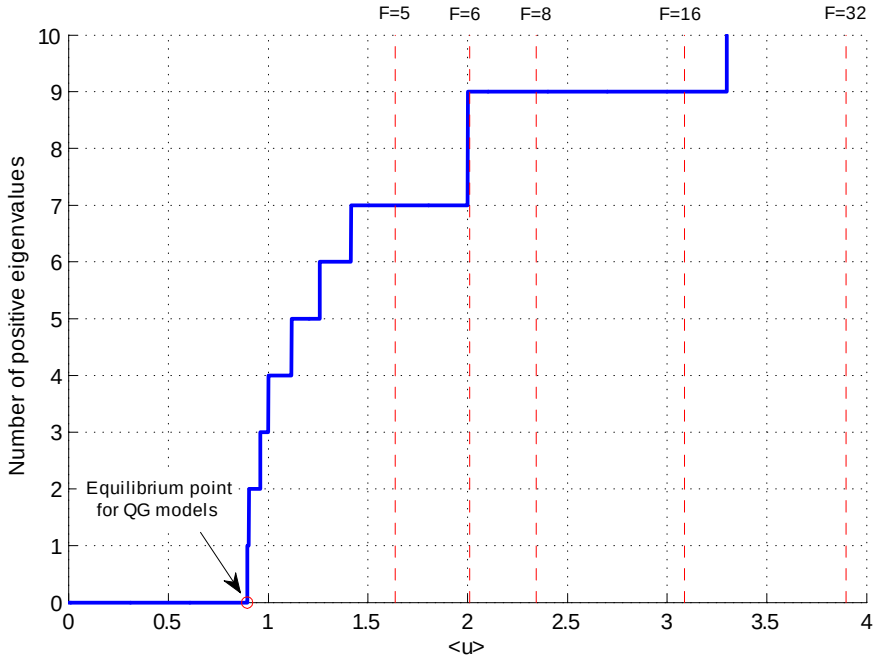

Figure 2: Number of positive eigenvalues of $L_v(\bar{\mathbf{u}})$ for L-96 with respect to the magnitude of the mean field $\bar{\mathbf{u}}$. The red dashed lines indicate exact equilibrium points for different value of the forcing parameter F. The green solid lines indicate equilibrium points for the DO UQ scheme for $N = 10$.

2. The important magnitude of $\bar{\mathbf{u}}$ leads to the activation of positive eigenvalues of $L_v(\bar{\mathbf{u}})$ (see Figure 2) that essentially absorb energy from the mean field and transform it to variance for the stochastic modes that are associated with this process.

3. The nonlinear conservative term $B(\mathbf{u}', \mathbf{u}')$ absorbs part of this energy, transfering it to the stable stochastic modes. It acts as dissipative mechanism for the unstable modes (balancing their positive eigenvalues) and external noise for the stable modes bringing all of them into a statistical equilibrium.

4. The stable modes receive energy from the unstable ones through the nonlinear conservative terms. A portion of this energy is dissipated and the rest is subsequently returned to the mean through the modes with negative eigenvalues. All modes including the mean flow dissipate energy through the negative definite part of the linearized dynamics.

This cycle of energy in the L-96 model is representative of any general model that contains i) unstable linearized modes whose stability depends on the mean field enegy level (i.e. that they absorb energy from the mean field), ii) stable modes, and iii) nonlinear conservative terms that transfer energy between the modes and through this tranfer the system is reaching an equilibrium. This structure is ubiquitous in turbulent systems in the atmosphere and ocean with forcing and dissipation [17, 14, 1, 2] as well as in fluid flows with lower dimensional attractors [15]. However, there are also examples of idealized truncated geophysical flows without dissipation and forcing with a Gaussian statistical equilibrium where the linear operator at the climate mean state is stable while the system has many positive Lyapunov exponents [13].

3 Limitations of Quasilinear Gaussian Closure for UQ in Unstable, Deterministic Systems

The simplest closure scheme [5] for the moment problem for a deterministic system stated in the previous section is to completely neglect in the evolution equation for the covariance the third-order moments, i.e. set $Q_F = 0$. This is equivalent with neglecting quadratic terms only in the equation for the covariance (partial linearization of the moment system) or by assuming Gaussian statistics. In this case the evolution of the covariance matrix is performed with the closed set of equations

$$\frac{d\bar{\mathbf{u}}}{dt} = [L + D]\,\bar{\mathbf{u}} + B(\bar{\mathbf{u}}, \bar{\mathbf{u}}) + R_{ij} B(\mathbf{v}_i, \mathbf{v}_j) + \mathbf{F} \tag{11a}$$

$$\frac{dR}{dt} = L_v R + R L_v^* \tag{11b}$$

In the second equation we observe that there are no terms that can express energy transfers between different modes of the system. Thus, for a turbulent system that means that if the energy level of the mean field is accurate we will have persistent instabilities that would cause uncontrollable growth of the unstable modes. This is also reflected from the non-existence of a steady state solution for the covariance equation (11b) if $\bar{\mathbf{u}}$ is such that $L_v(\bar{\mathbf{u}})$ has positive eigenvalues. For the L-96 system this will not be the case since the QG closure scheme avoids blow-up of the unstable modes by reducing the mean field energy to a level that the linearized operator has zero number of eigenvalue pairs with positive real part (see Figure 2) so that the energy flowing from the mean to the unstable modes is balanced by the dissipation of energy occurring in the unstable modes (no

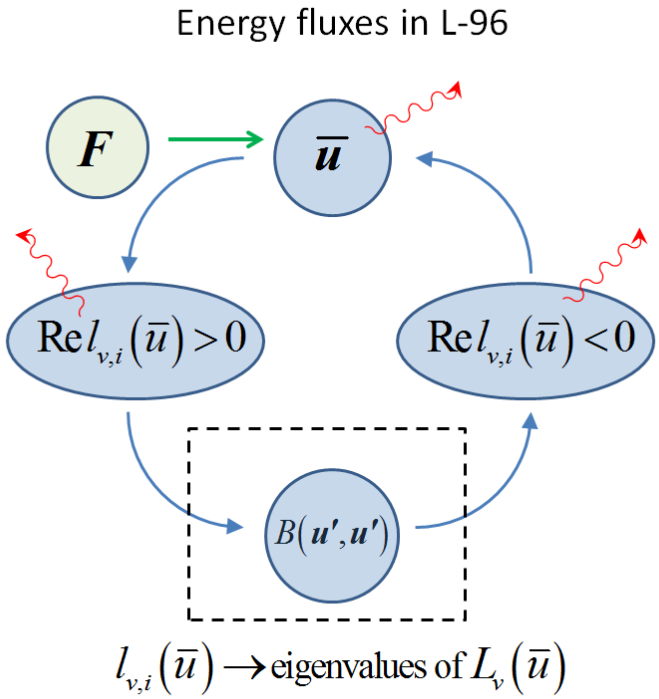

Figure 3: Energy flow in the L-96 system. Energy flows from the mean field to the linearly unstable modes and then redistributed through nonlinear, conservative terms to the stable modes. Red arrows denotes dissipation, while the dashed box indicates terms that conserve energy.

energy is transferred to the stable modes). Note that this behavior is independent of the forcing parameter value F as long as the latter is sufficiently large in order for the exact solution to have non-zero number of positive eigenvalues. In fact, this behavior can be demonstrated rigorously for the L-96 model as sketched below.

We consider homogeneous statistical solutions defined by the deterministic Gaussian closure in (11a)-(11b) for the L-96 model. With these homogeneous assumptions, the mean, $\bar{\mathbf{u}}(t)$, is a time varying constant, the covariance multiplier is diagonal in Fourier space, $R = r_j \delta_{ij}$, and the linear operator, L_v, is the diagonal Fourier multiplier [13, 9]

$$L_v r_j = l_j r_j$$

with

$$l_j(\bar{u}) = \left(e^{\frac{j}{J} 2\pi i} - e^{-\frac{j}{J} 4\pi i}\right) \bar{u} - 1, \quad \text{for} \quad j \leq \frac{J}{2} \quad \text{with } J = 40. \tag{12}$$

The exact solution of the quasilinear Gaussian closure equations in (11a)-(11b) for the L-96 model with these homogeneity assumptions becomes the diagonal equations,

$$\begin{aligned} \frac{dr_j}{dt} &= 2 \operatorname{Re} l_j(\bar{u})\, r_j \\ \frac{d\bar{u}}{dt} &= -\bar{u} + F + \sum_{j=0}^{20} r_j B(\mathbf{v}_j, \mathbf{v}_j).\mathbf{v}_0 \end{aligned}$$

with $\mathbf{v}_j$ the $j-$th Fourier eigenmode; it is easy to check that $B(\mathbf{v}_j, \mathbf{v}_j).\mathbf{v}_0 \neq 0$ for any $j \neq 0$. With equations (12) and (13) we find trivially that the statistical steady state of the deterministic Gaussian closure for a given $\bar{u}_\infty$ require

$$r_{j,\infty} = 0 \quad \text{unless} \quad \operatorname{Re} l_j(\bar{u}) = 0 \tag{14}$$

i.e. the covariance is restricted to the neutrally stable modes of L_v at $\bar{\mathbf{u}}_\infty$.Furthermore, clearly the first equations in (13) have a dynamically stable statistically steady state according to linear theory only if $\operatorname{Re} l_j(\bar{u}) \leq 0$, i.e. $L_v(\bar{\mathbf{u}}_\infty)$ has no unstable eigenmodes. Thus, the only allowed stable statistical steady states of the Gaussian closure are defined by the unique value $\bar{u}_{cr}$, satisfying marginal linear stability as depicted at the bottom of Figure 2 where for any F, the variance $r_{j,\infty}$ at the neutrally stable mode is adjusted so that

$$\bar{u}_{cr} = F + \sum_{j=0}^{20} r_{j,\infty} B(\mathbf{v}_j, \mathbf{v}_j).\mathbf{v}_0$$

i.e. the right hand side of the second equation in (13) also vanishes.

This indicates the fundamental limitations of the straightforward Gaussian closure for unstable deterministic dynamical systems. On the other hand, for some nonlinear systems with intermittent transient instabilities, such simple quasilinear Gaussian closures augmented by suitable stochastic forcing can have remarkable skill for UQ in turbulent systems [3, 10]. An alternative procedure often used in the geophysical turbulence literature is to ignore the feedback to the mean flow and stabilize the instabilities in the fluctuations from (11b) by adding adhoc dissipation and white noise forcing [4]; the limitations of these methods for UQ in the present context are discussed below and earlier elsewhere [11, 10, 3].

4 Modified Quasilinear Gaussian (MQG) models

From the previous analysis it is clear that the inclusion of an energy transfer mechanism that will continuously transfer energy from the unstable modes to the stable ones is essential in order to achieve the correct energy levels in the system. Our goal is to build a time-dependent dynamical system that retains these energy transfers at steady state while it is minimally modified so that it has good UQ properties for the transient part of the response and for modified external parameters.

Including a constant $Q_{F,\infty}$ that has been computed using steady state information of the system statistics will not resolve the issue since the eigenvalues of L_v will make the steady state solution of the covariance equation

$$\frac{dR_\infty}{dt} = 0 = L_v R_\infty + R_\infty L_v^* + Q_\sigma + Q_{F,\infty}$$

unstable for a mean field that has the correct energy level, i.e. the pair R_∞, $\bar{\mathbf{u}}_\infty$ will be an unstable steady state solution if the nonlinear fluxes are represented as a constant matrix $Q_{F,\infty}$.

Based on the observation that the eigenvalues are effectively changed by the existence of the nonlinear energy transfer mechanism we propose a special form of the flux Q_F that will make the correct steady state statistics a stable equilibrium. More specifically we split the nonlinear fluxes into a positive semi-definite part Q_F^+ and a negative semi-definite part Q_F^- :

$$Q_F = Q_F^- + Q_F^+.$$

Note that the nonlinear fluxes should always satisfy the conservative property of B which in the above context is expressed by the constraint (8):

$$Tr\left[Q_F\right] = 0 \Rightarrow Tr\left[Q_F^+\right] = -Tr\left[Q_F^-\right]. \tag{15}$$

The positive fluxes Q_F^+ indicate the energy being 'fed' to the stable modes in the form of external stochastic noise. On the other hand the negative fluxes Q_F^- should act directly on the linearly unstable modes of the spectrum, effectively stabilizing the unstable modes. To achieve this we choose to represent the negative fluxes as

$$Q_F^-\left(R\right) = N_\infty R + R N_\infty^* \tag{16}$$

with N_∞ determined by solving the equation

$$Q_{F\infty}^- = Q_F^-\left(R_\infty\right) = N_\infty R_\infty + R_\infty N_\infty^* \tag{17}$$

where $Q_F^-\left(R_\infty\right)$ is the negative semi-definite part of the steady-state fluxes obtained by the equilibrium equation $Q_{F\infty} = -L_v\left(\bar{\mathbf{u}}_\infty\right) R_\infty - R_\infty L_v^*\left(\bar{\mathbf{u}}_\infty\right)$. Equation (17) essentially connects the negative-definite part of the nonlinear energy fluxes (which is a functional of the third-order statistical moments) with the second-order statistical properties that express energy properties of the system.

We can easily verify that N_∞ in equation (17) will be given explicitely by

$$N_\infty = \frac{1}{2} Q_F^-\left(R_\infty\right) R_\infty^{-1}.$$

On the other hand the positive fluxes Q_F^+ will be computed also according to the steady state information, i.e. based on the positive semi-definite fluxes $Q_{F\infty}^+ = Q_F^+\left(R_\infty\right)$. The form of this

matrix defines the amount of energy that the linearly stable modes should receive in the form of additive noise.

The conservative property of the nonlinear energy transfer operator B requires that for all times the conservation property (15) is satisfied. This is achieved by retaining the shape of the fluxes (i.e. distribution among different modes) but rescaling their magnitudes so that (15) is achieved. This can be obtained by choosing the positive fluxes as

$$Q_F^+ = -\frac{Tr\left[Q_F^-\right]}{Tr\left[Q_{F\infty}^+\right]} Q_{F\infty}^+. \tag{18}$$

The last formulation guarantees the conservation property (15) at every instant of time. In this way we substitute the nonlinear conservative mechanism by a conservative pair of positive and negative energy fluxes having the form of additional damping for the unstable modes and additive noise for the stable modes (Figure 4). This is the minimal amount of additional damping and noise required in order to achieve correct steady state statistics, thus we have a minimally changed model compared to the original equation. As we will see in the next sections, this minimal modification allows for very good UQ properties even in the transient phase of the response with suitable nonlinear dynamics in time.

Note that all of the required fluxes $Q_{F\infty}^-$, $Q_{F\infty}^+$ are evaluated explicitely from available information involving the linear operator, $L_v\left(\bar{\mathbf{u}}_\infty\right)$, and the covariance matrix, R_∞ in a statistical steady state. In addition, since the nonlinear flux model is kept separate from the unmodified linear dynamics, it expresses an inherent property of the system, a direct link between second and third-order statistical moments in the same spirit that Karman-Howarth equation [6] does for isotropic turbulence. Next we develop a transient dynamical model which has these statistics as a stable fixed point.

4.1 Improving marginal stability of the stochastic attractor

We saw that the negative fluxes Q_F^- essentially equilibrate the unstable directions of the linearized dynamics. The equilibration is performed in the steady state by suitably choosing the additional damping N so that the total energy fluxes (linear and nonlinear) involving these modes is vanishing in the statistical steady state. Even though the correct steady state is achieved the necessary time for this equilibration is infinite since this approach of modeling the nonlinear fluxes results in marginally stable equilibrium.

To avoid this difficulty we add uniformly a small amount of dissipation and noise over all modes so that the attractor in the steady state remains invariant. This can always be done if we choose

$$N_\infty = \frac{1}{2}\left(Q_{F\infty}^- - qI\right) R_\infty^{-1} \tag{19}$$

$$Q_F^+ = -\frac{Tr\left[Q_F^-\right]}{Tr\left[Q_{F\infty}^+\right]}\left(Q_{F\infty}^+ + qI\right) \tag{20}$$

where q is a positive constant. For the problem that we consider we choose to scale this with the maximum eigenvalue of the steady state fluxes, i.e. we set

$$q = d_s \lambda_{\max}\left[Q_{F\infty}\right].$$

Following this approach we avoid the problem of marginally stable equilibrium and we increase significantly the skill of the UQ scheme even for very small values (but non-zero) of the constant

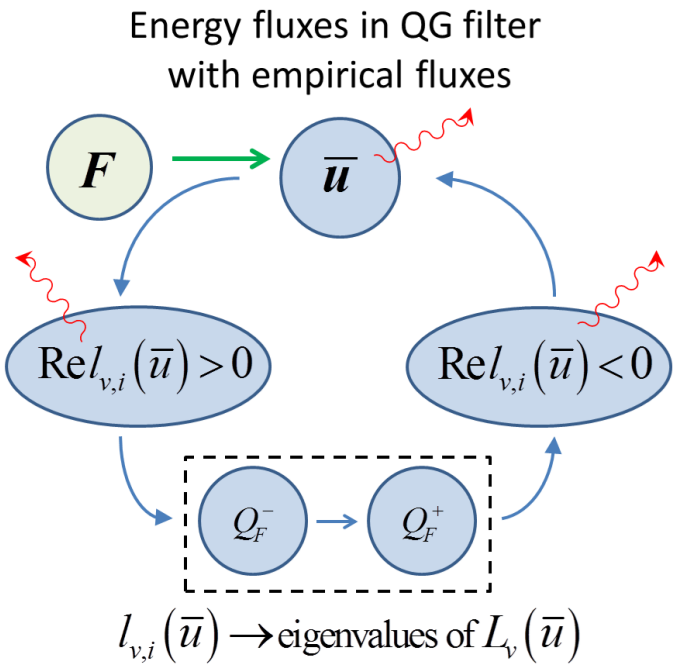

Figure 4: Energy flow in the QG-ES filter. Energy flows from the mean field to the linearly unstable modes and then redistributed through empirical, conservative fluxes to the stable modes. Red arrows denotes dissipation, while the dashed box indicates terms that conserve energy.

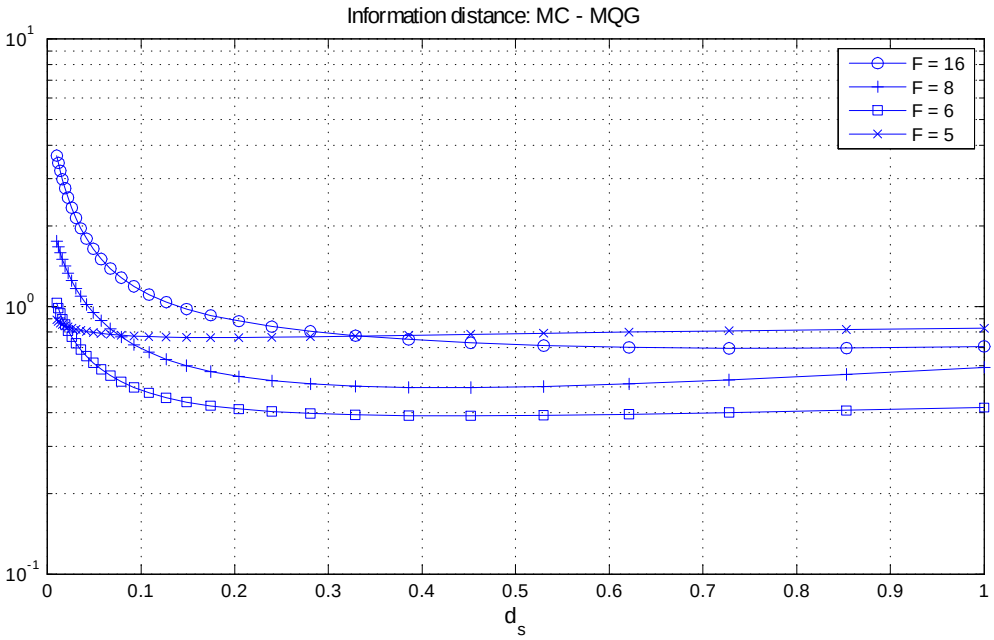

Figure 5: Information distance between Monte-Carlo solution and MQG UQ scheme for different values of the parameter d_s and over different dynamical regimes of the L96 system.

d_s. In Figure 5 we present results for the L-96 system in terms of the the information distance [10] between the Monte-Carlo solution and the MQG solution over different values of the parameter d_s and forcing F. To compute the information distance we use only second order information since MQG does not provide hogher order statistics:

$$\begin{aligned}\mathcal{P}=&\frac{1}{2}\left(\bar{\mathbf{u}}^*_{MQG}-\bar{\mathbf{u}}^*_{MC}\right)R^{-1}_{MC}\left(\bar{\mathbf{u}}_{MQG}-\bar{\mathbf{u}}_{MC}\right)\\&+\left[-\frac{1}{2}\log\det R_{MQG}R^{-1}_{MC}+\frac{1}{2}tr\left(R_{MQG}R^{-1}_{MC}\right)-M\right]\end{aligned}$$

We observe that for the chaotic regimes ($F=5,6$) the skill of the MQG scheme is not influenced very strongly from the choice of the parameter d_s as long as this is not zero. In this regime d_s behaves essentially as a singular parameter. For much larger values of d_s the performance slowly deteriorates since the linear and nonlinear energy fluxes are 'buried' by the uniform diagonal part qI. For larger values of F the transition (to very good performance) is much smoother. In all dynamical regimes we see that the dependence of the performance of the UQ scheme on the exact value of d_s is very weak as long as this value is non zero.

4.2 Scaling of the nonlinear energy fluxes and transient dynamics for MQG

To achieve the best possible accuracy in the timescales of the system, we parametrize the matrix N_∞ by various forms of the energy or rates of energy flux. In particular from (7) we have the dimensional relation that $N \sim \sigma_i$ Based on this we use the following form

$$N = \frac{f(R, L_v)}{f(R_\infty, L_{v\infty})} N_\infty \qquad \text{where} \qquad N_\infty = \frac{1}{2}\left(Q^-_{F\infty} - qI\right) R_\infty^{-1} \tag{21}$$

with the function $f(R, L_v)$ given by

$$\begin{aligned}
f(R) &= \left[Tr(R)\right]^{\frac{1}{2}}, && \text{Energy functional} \\
f(R, L_v) &= \left[\sum_{\lambda_i[L_v]>0} \sigma_i^2\right]^{\frac{1}{2}}, && \text{Energy of unstable modes} \\
f(R) &= \sum_{i=1}^{N} \sigma_i, && \text{Sum of typical deviations} \\
f(R, L_v) &= \sum_{\lambda_i[L_v]>0} \lambda_i[L_v]\, \sigma_i, && \text{Sum of positive nonlinear fluxes}
\end{aligned}$$

where σ_i^2 are the eigenvalues of the covariance matrix R. As shown in a non-trivial test example for L-96 in Figure (6) below, the form of f strongly influences the transient behavior. Compared with the other choices, the best one is always the sum of typical deviations and for this reason it will be the standard choice for what follows.

4.3 Summary of MQG and a related stochastic ODE

With all of the above discussion, the Modified Quasilinear Gaussian closure (MQG) developed above and implemented in the section 5 below is given by the nonlinear dynamical system for the mean and covariance,

$$\frac{d\bar{\mathbf{u}}}{dt} = [L + D]\,\bar{\mathbf{u}} + B(\bar{\mathbf{u}}, \bar{\mathbf{u}}) + R_{ij} B(\mathbf{v}_i, \mathbf{v}_j) + \mathbf{F} \tag{22a}$$

$$\frac{dR}{dt} = L_v R + R L_v^* + N R + R N^* + Q_F^+ + Q_\sigma \tag{22b}$$

where

$$N = \frac{f(R)}{f(R_\infty)} N_\infty \quad \text{with} \quad N_\infty = \frac{1}{2}\left(Q^-_{F\infty} - qI\right) R_\infty^{-1} \quad \text{and} \quad f(R) = \sum_{i=1}^{N} \sigma_i, \tag{23a}$$

$$Q_F^+ = -\frac{Tr\left[Q_F^-\right]}{Tr\left[Q^+_{F\infty}\right]}\left(Q^+_{F\infty} + qI\right) \quad \text{with} \quad Q_F^- = NR + RN^*, \tag{23b}$$

$$q = d_s \lambda_{\max}\left[Q_{F\infty}\right] \quad \text{with} \quad d_s \ll 1. \tag{23c}$$

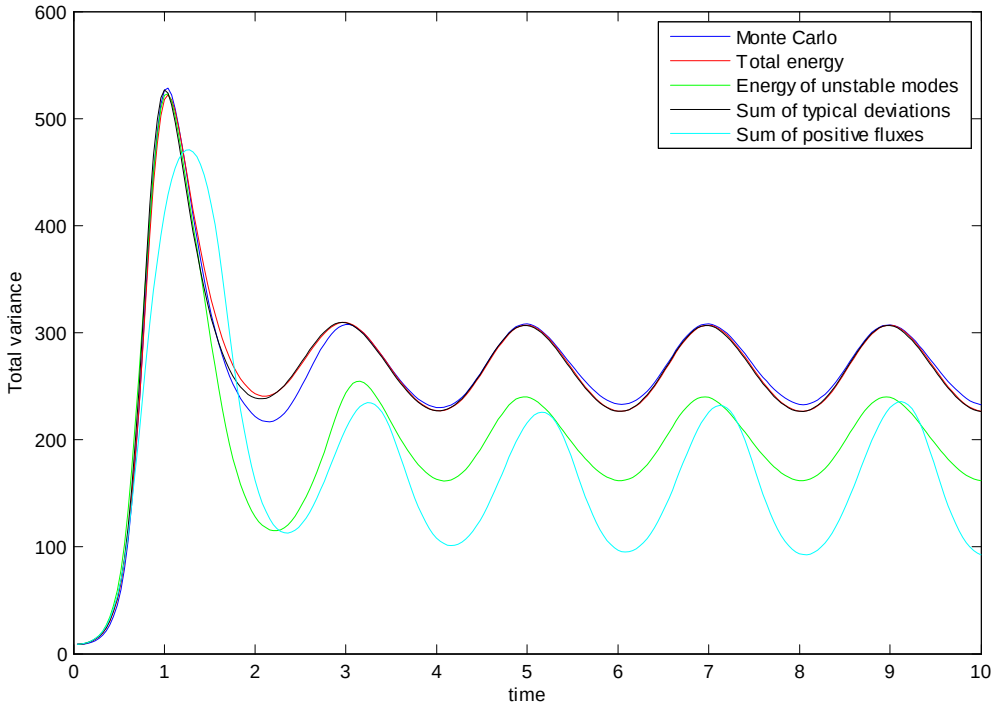

Figure 6: Comparison of total variance over different scalings of the energy fluxes. The case considered here is the Lorenz 96 system with $F = 8 + \sin(\pi t)$.

It is interesting to ask if there is a formal nonlinear stochastic equation which has the mean and covariance matrix in (22), i.e. formally, the closed system of SDE's has the mean and covariance agreeing with (22). Next we proceed to the formulation of a stochastic differential equation that is equivalent to the closed system of equations describing the mean and covariance of the MQG closure scheme.

$$\frac{d\bar{\mathbf{u}}}{dt} = [L+D]\,\bar{\mathbf{u}} + B(\bar{\mathbf{u}},\bar{\mathbf{u}}) + \overline{B\left(\mathbf{u}',\mathbf{u}'\right)} + \mathbf{F}$$
$$\frac{d\mathbf{u}'}{dt} = \left([L+D]\,\mathbf{u}' + B\left(\bar{\mathbf{u}},\mathbf{u}'\right) + B\left(\mathbf{u}',\bar{\mathbf{u}}\right)\right) + N\left(\overline{\mathbf{u}'\mathbf{u}'^{*}},\bar{\mathbf{u}}\right)\mathbf{u}' + \left[Q_F^{+}\left(\overline{\mathbf{u}'\mathbf{u}'^{*}},\bar{\mathbf{u}}\right)\right]^{\frac{1}{2}}\dot{\mathbf{W}}_1 + \sigma\dot{\mathbf{W}}_2$$

where N, Q_F^+ are defined by equations (21) and (20). By direct comparison with the exact equations (2), (3) we see that the mean equation is identical while the equation for the stochastic perturbation differs in the nonlinear term. In particular the quadratic term of the exact equation has been replaced by a pair of damping and noise terms which depend linear on the state of the perturbation and non-linearly, non-locally to the second order statistics of the systems. Nonlocallity is meant in the sense that the damping coefficient depend on spatial functionals of the covariance function.

Note that the above set cannot be merged into a single equation since the modification of the quadratic terms has occurred only in the perturbation equation while the equation for the mean remains invariant. We emphasize that the constructed set of closed equations is a representative of a new class of stochastic differential equations where the evolution of each stochastic realization depends on the global statistics, i.e. on the collective or statistical behavior of all the realizations. In particular, the associated formal Fokker-Planck equation is nonlinear. Such novel stochastic equations merit further mathematical study.

5 Illustration and validation in the L-96 model

In this section we will illustrate numerically the UQ properties of the MQG closure. We first study the performance of the UQ scheme for the case of constant in time forcing parameter F. The nonlinear fluxes N_∞, Q_F^+ are specified using, for each case of forcing parameter F, the steady state covariance and mean: R_∞, $\bar{\mathbf{u}}_\infty$. The scaling of the nonlinear fluxes is done using the sum of the typical deviations as described above.

The results are shown in Figure 7 for four different forcing parameters (four columns) covering all three dynamical regimes of L-96. In particular for $F = 16$ we observe that energy is distributed along every wavenumber while for the weakly chaotic regime corresponding to $F = 5$ the spectrum has a much sharper form with a well distinguished peak. The skill of the MQG closure scheme is illustrated both from its ability to reproduce in a stable way the linearly unstable, steady-state attractor but also from its skill during the transient phase.

More specifically, we can observe the multiscale character of the response involving initially a rapid growth of almost every mode and subsequently a multiscale relaxation to the equilibrium spectrum. The initial conditions of the system are shown in the bottom row - in all cases we initialize uncertainty in the high frequency modes - the mean is also initiated as constant. The MQG algorithm is capturing both the initial rapid growth of the energy and mean but also the subsequent slow dynamics. The case $F = 5$ is particularly difficult because the high energy modes require a substantial amount of time to equilibrate. Despite this multiscale character of the stochastic response the MQG scheme is able to recover both fast and slow dynamics of the system, as can be

seen directly from the comparison of the spectra. We emphasize that in all the considered cases the system is initiated very far from equilibrium and performs strongly nonlinear energy oscillations over all wavenumbers until it reaches an equilibrium. These oscillations create energy levels for the mean and the perturbations which are much higher than the corresponding equilibrium values.

The second numerical experiment that we perform is one with time periodic forcing parameter F. The comparison of MQG with Monte-Carlo can be seen in Figure 8 where we observe that because of the time dependent character of the excitation, the system converges to a time-periodic stochastic attractor. For each case the nonlinear fluxes are computed based on the exact steady state statistics of the system that correspond to the time-averaged value of the excitation parameter (these time averaged values are the same with those shown in Figure 7, i.e. $\bar{F} = 16,\ 8,\ 6,\ 5$). In all cases the performance of the MQG scheme on capturing the time-periodic stochastic attractor is remarkable. We also perform the same numerical experiment using aperiodic forcing parameters generated by the Ornstein–Uhlenbeck process

$$dF = -\frac{1}{\tau_F} F dt + \sigma_F dW$$

Similarly with the time periodic case the random realizations of the forcing parameters have averaged values: $\bar{F} = 16,\ 8,\ 6,\ 5$. These time-constant cases are used as sources of steady-state statistics for the nonlinear fluxes employed in the aperiodic forcing parameter cases. The results are shown in Figure 9 where it is illustrated that the exact and approximate statistics compare favorably. Note that for $\bar{F} = 16$ a different kind of initial spectrum is considered in order to illustrate the robustness of performance over different intial spectra.

Finally, in order to push the developed UQ scheme to its limits we consider an aperiodic forcing parameter that has very strong fluctuations ranging from $F = 0$ to $F = 30$. In addition, the forcing is no more spatially constant but instead it is non-zero in the spatial nodes $j = 1, ..., 20$ and zero in the nodes $j = 21, ..., 40$. The nonlinear fluxes are computed based on steady state statistics for $F = 10$. We recall that for F close to zero L-96 has no unstable directions while for $F = 30$ it has more than ten unstable wavenumbers. We observe in Figure 10 that while there are some discrepancies, especially when the forcing parameter takes its maximum value, MQG is successful on capturing the very strong variations of energy even in a mode-by-mode comparison. We emphasize that this is not a spatially homogeneous case as the previous examples.

Comparison with Mean Stochastic Models (MSM)

A very common UQ strategy in the turbulence modeling in climate science [4, 12, 11] is based on the substitution of the nonlinear terms in the quadratic system by linear terms which are tuned so that the correlation time scale for each mode, as well as its steady state variance, coincide with the exact steady-state values which are assumed to be known. More specifically, the fluctuations in the original dynamical system are approximated by a linear system of the form

$$\frac{d\mathbf{u}}{dt} = (L + D + G)\,\mathbf{u} + B\left(\bar{\mathbf{u}}_\infty, \mathbf{u}\right) + B\left(\mathbf{u}, \bar{\mathbf{u}}_\infty\right) + \mathbf{F}\left(t\right) + \sigma\dot{\mathbf{W}}_1 + \rho\dot{\mathbf{W}}_2,$$

where the augmented damping and white noise forcing G and ρ are chosen to roughly produce the correct steady state variance and correlation time scales. In general there are no explicit choices of G and ρ which can exactly match the logged correlation and covariances exactly [11, 4]. Nevertheless such methods qualitatively reproduce the features of synoptic scale eddies in the atmosphere [4];

such methods can also be very skillful as filters with judicious model error [12]. However, they are severely deficient as UQ schemes [11, 10, 3] since, for example, they cannot capture the change in variance due to external forcing. Mean stochastic models, MSM-1, based on the climate variances and integral of the autocorrelation (and which are always realizable), and models, MSM-2, based on the standard procedure [4] sketched above have been developed for the L-96 model [11, 12].

In Figure 11 we present a direct comparison in terms of the total energy of the mean and random part of the stochastic solution for the L-96 system with a time dependent forcing parameter (the same forcing parameter with Figure 9 - first column). As expected from the theoretical results, both MSM models do not capture any fluctuations on the covariance of the solution caused by the time-dependent nature of the forcing parameter. Clearly, this has very important consequences on the estimation of the mean as well. The failure of both models is due to the fluctuations of the forcing parameter that push the system to different dynamical regimes, while MSM schemes are tuned for a specific forcing value and their performance drops drastically when the quality of the dynamics (number of unstable directions, shape of the spectrum, timescales) changes significantly. As we justified both theoretically and numerically this is not the case for the MQG scheme where the nonlinear fluxes are modeled as the minimum amount of noise and damping required to represent these nonlinear fluxes, while the linear (and possibly unstable) dynamics of the system remain unchanged.

6 Concluding discussion and future directions

We have analyzed energy transfer properties in high-dimensional quadratic systems and based on this analysis we have developed a novel, second-order, closure scheme for uncertainty quantification. More specifically, in the first part of this work we have illustrated the synergistic activity of persistent linear instabilities with a nonlinear energy transfer mechanism that results in finite amount of energy in both the unstable (which would blow-up otherwise) and stable modes (which would have zero energy otherwise). This combined effect has as a result the distribution of important amount of energy over all the modes of the system, creating turbulent responses.

Using these dynamical properties we have illustrated the fundamental limitations of closure schemes that ignore or partially model the nonlinear interactions between modes. More specifically, we have rigorously proven that UQ methods that ignore third-order moments (such as quasilinear Gaussian closure) will equilibrate only if the mean has sufficiently low energy so that all the modes are either stable or neutrally stable. This is because in the absence of nonlinear energy transfers an unstable mode will lead to variance blow-up. Therefore, QG models will systematically fail to perform uncertainty quantification in turbulent systems characterized by persistent instabilities.

The second part of the paper involves the explicit modeling of these nonlinear interactions. This is done by using exact, second-order, steady state information that leads to explicit modeling of the nonlinear energy transfers in the form of additional damping for the linearly unstable modes and external stochastic noise for the stable modes. Essentially we are using second-order information for the steady state statistics to quantify the collective effect of all third order moments on the energy fluxes in a wide variety of different chaotic regimes both for statistical initial data far from equilibrium and for randomly fluctuating extreme forcing. This judicious modeling of the energy transfer mechanism allows for the MQG scheme to capture robustly the linearly unstable steady state of the original system. Moreover, by parametrizing the magnitude of the nonlinear fluxes with spatial functionals of the modes instantaneous energy we are able to obtain remarkable skill even for the transient phase of the response. The performance of the UQ scheme is illustrated through

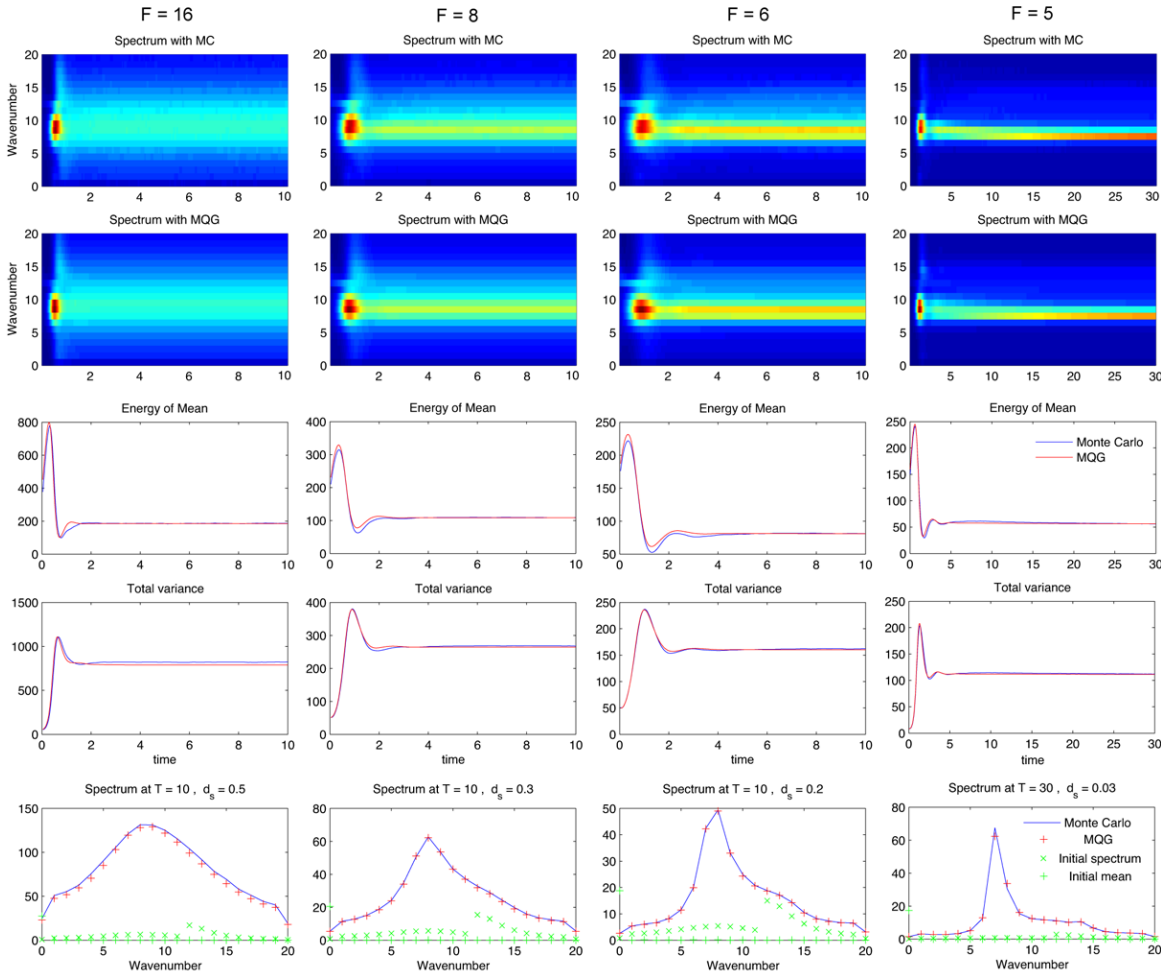

Figure 7: Comparison of MQG uncertainty quantification scheme with exact statistics produced by Monte-Carlo method. Results are shown for different values of the forcing parameter F (contant in time) corresponding to weakly chaotic, chaotic, and turbulent regimes.

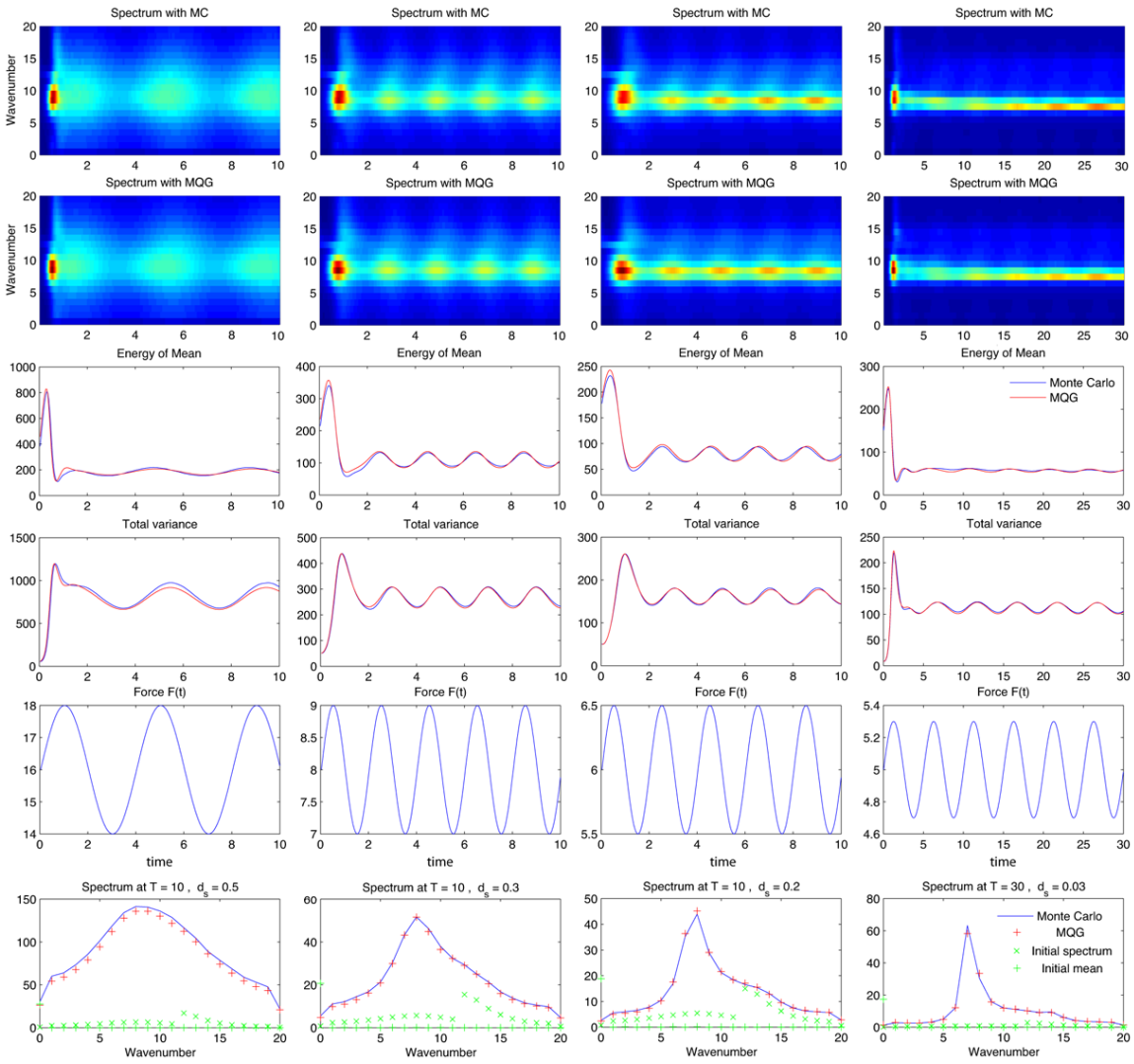

Figure 8: Comparison of MQG uncertainty quantification scheme with exact statistics produced by Monte-Carlo method. Results are shown for different dynamical regimes of the time-periodic forcing parameter F. The nonlinear fluxes have been computed using the time averaged value of $F(t)$ - these averaged values coincide with the constant values of the previous Figure.

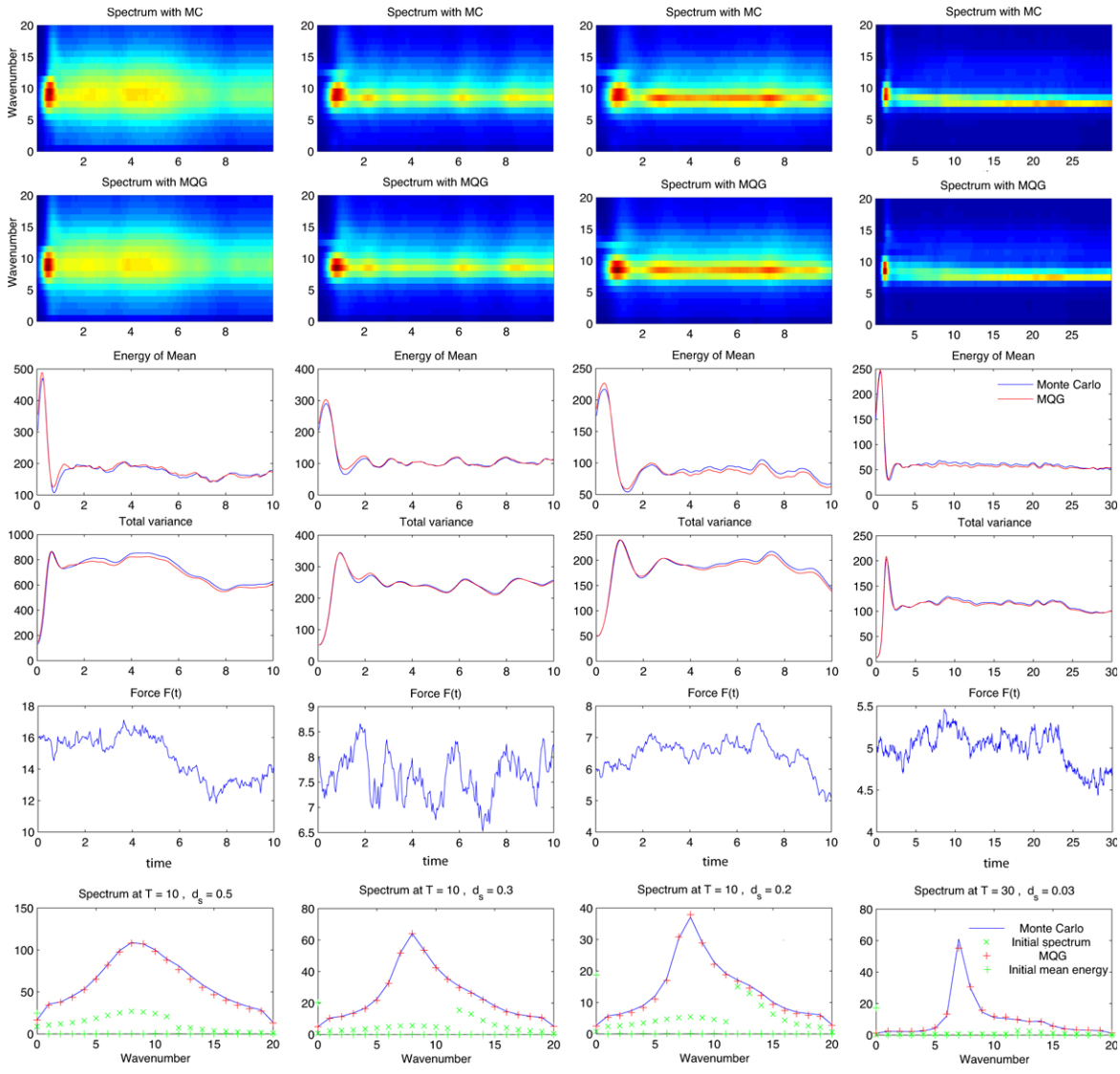

Figure 9: Comparison of MQG uncertainty quantification scheme with exact statistics produced by Monte-Carlo method. Results are shown for different dynamical regimes of the aperiodic forcing parameter F generated as an Ornstein–Uhlenbeck process. The nonlinear fluxes have been computed using the time averaged value of $F(t)$ - these averaged values coincide with the constant values of Figure 7. Note that for $\bar{F} = 16$ a different kind of initial conditions is considered.

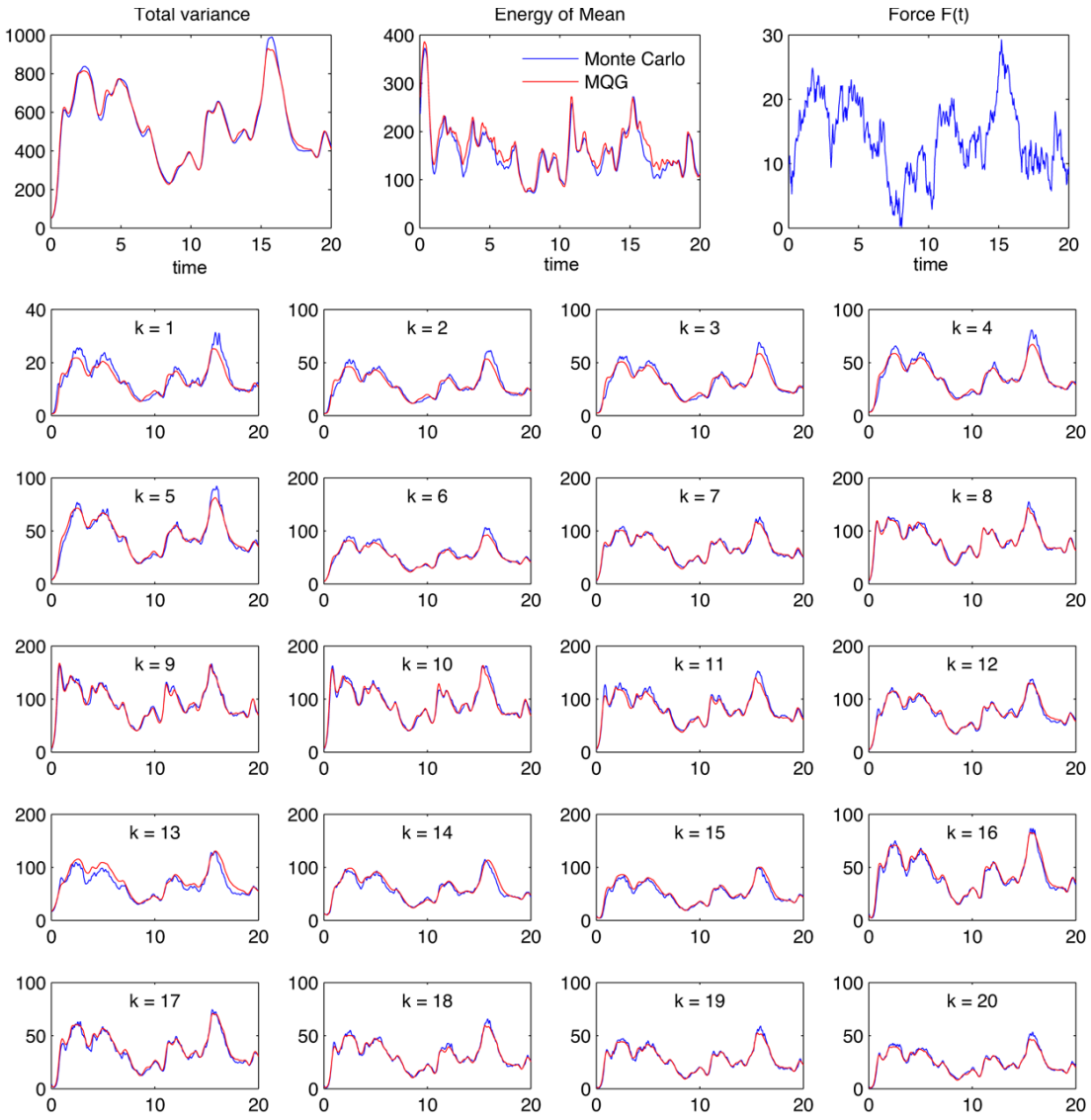

Figure 10: Comparison of MQG with direct Monte Carlo for time dependent forcing parameter $F(t)$ excibiting very strong variations covering all dynamical regimes: deterministic $(F < 1)$, chaotic, and turbulent. The nonlinear fluxes have been computed using the steady state spectrum and mean for $F = 10$.

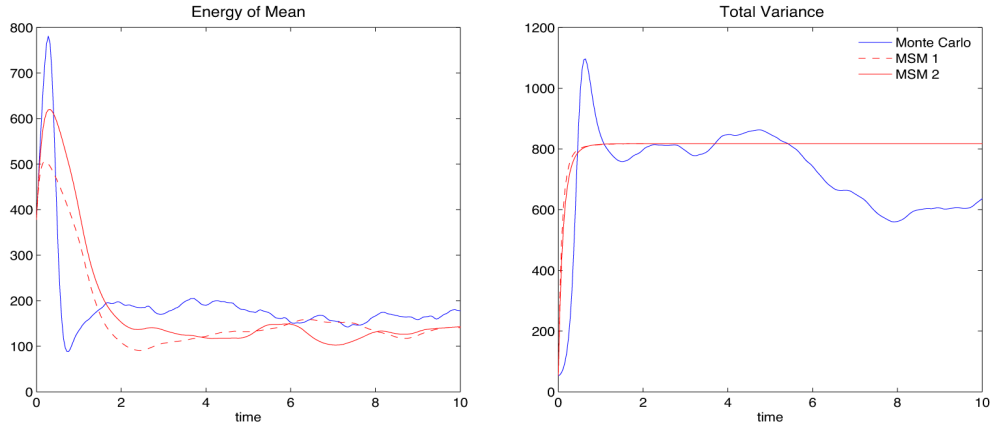

Figure 11: Comparison of MSM 1 and 2 with Monte-Carlo method for the same time-dependent forcing of Figure 9 (first column).

the L-96 system which, despite its simple formulation, is a paradigm model that exhibits strongly unstable and turbulent dynamics. The derived UQ scheme maintains its skill even for the case of time-dependent excitation when the system is pushed in dynamical regimes which are completely different from the regime used to quantify the nonlinear interactions. These encouraging results suggest future applications of MQG to more realistic turbulent geophysical systems [14, 17].

Despite the remarkable skill of MQG method for systems with persistent instabilities it is important to keep in mind that it provides only second-order statistics for the response, even though it indirectly uses higher-order stochastic information in its calibration. In addition, its applicability is limited to stochastic excitations which have similar spatial structure with the stochastic excitation for which the nonlinear fluxes have been estimated. Both of these limitations may be resolved by combining global UQ methods that can 'see' and resolve the full turbulent spectrum (such as MQG) with order-reduction approaches such as dynamically orthogonal field equations that allow for higher statistical order, spatiotemporal modeling only along specific directions [16, 15]. Current research work by the authors involves the blending of these two methodologies, in order to capture accurately both the energy spectrum as well as the higher-order statistical structure in important subspaces, and results will be presented in the near future.

Acknowledgment. The research of A. Majda is partially supported by NFS grant DMS-0456713, NSF CMG grant DMS-1025468, and ONR grants ONR-DRI N00014-10-1-0554 and N00014-11-1-0306. T. Sapsis is supported as postdoctoral fellow on the first and last grand.

References

[1] R. V. Abramov and A. J. Majda, *New algorithms for low frequency climate response*, J. Atmos. Sci., 66 (2009), pp. 286–309.

[2] ——, *Low frequency climate response of quasigeostropic wind-driven ocean circulation*, Journal of Physical Oceanography, 42 (2011), pp. 243–260.

[3] M. Branicki and A. J. Majda, *Quantifying uncertainty for climate change and long range forecasting scenarios with model errors. non-guassian models with intermittency*, Nonlinearity, (2012), p. Submitted.

[4] T. DelSole, *Stochastic models of quasigeostrophic turbulence*, Surv. Geophys., 25 (2004), pp. 107–149.

[5] E. Epstein, *Stochastic dynamic predictions*, Tellus, 21 (1969), pp. 739–759.

[6] U. Frisch, *Turbulence, The Legacy of A. N. Kolmogorov*, Cambridge University Press, 1996.

[7] E. Lorenz, *Predictability - a problem partly solved*, in Proceedings on Predictability, ECMWF, September 1996, pp. 1–18.

[8] E. N. Lorenz and K. A. Emanuel, *Optimal sites for supplementary weather observations: Simulations with a small model*, J. Atmos. Sci., 55 (1998), pp. 399–414.

[9] A. J. Majda, R. V. Abramov, and M. J. Grote, *Information Theory and Stochastics for Multiscale Nonlinear Systems*, vol. 25 of CRM Monograph Series, American Mathematical Society, 2005.

[10] A. J. Majda and M. Branicki, *Lessons in uncertainty quantification for turbulent dynamical system*, Discrete and Continuous Dynamical Systems, 32 (2012), pp. 3133–3221.

[11] A. J. Majda, B. Gershgorin, and Y. Yuan, *Low-frequency climate response and fluctuation-dissipation theorems: Theory and practice*, J. Atmos. Sci., 67 (2010), pp. 1186–1201.

[12] A. J. Majda and J. Harlim, *Filtering Complex Turbulent Systems*, Cambridge University Press, 2012.

[13] A. J. Majda and X. Wang, *Nonlinear Dynamics and Statistical Theories for Basic Geophysical Flows*, Cambridge University Press, 2006.

[14] R. Salmon, *Lectures on Geophysical Fluid Dynamics*, Oxford University Press, 1998.

[15] T. P. Sapsis, *Inertial manifold dimensionality and finite-time instabilities in infinite-dimensional systems with applications to 2d navier-stokes equations*, submitted, (2011).

[16] T. P. Sapsis and P. F. J. Lermusiaux, *Dynamically orthogonal field equations for continuous stochastic dynamical systems*, Physica D, 238 (2009), pp. 2347–2360.

[17] S. Smith, G. Boccaletti, C. Henning, I. Marinov, C. Tam, I. Held, and G. Vallis, *Turbulence diffusion in the geostrophic inverse cascade*, Journal of Fluid Mechanics, 469 (2002), pp. 13–48.